SIRT1 facilitates primordial follicle recruitment independent of deacetylase activity through directly modulating *Akt1* and *mTOR* transcription

Tuo Zhang[#1], Xinhua Du[#1], Lihua Zhao[#2,1], Meina He[1], Lin Lin[1], Chuanhui Guo[1], Xinran Zhang[1], Jun Han[1], Hao Yan[1], Kun Huang[1], Guanghong Sun[1], Lei Yan[3], Bo Zhou[1], Guoliang Xia[1,4], YingYing Qin*[3], Chao Wang*[1]

[1]State Key Laboratory of Agrobiotechnology, College of Biological Sciences, China Agricultural University, Beijing 100193, China

[2]Department of Pathology and Hepatology, the 5th Medical Centre, Chinese people's Liberation Army General Hospital, Beijing 100039, China

[3]Center for Reproductive Medicine, Shandong Provincial Hospital Affiliated to Shandong University; National Research Center for Assisted Reproductive Technology and Reproductive Genetics; The Key Laboratory of Reproductive Endocrinology (Shandong University), Ministry of Education; Shandong Provincial Key Laboratory of Reproductive Medicine, Jinan 250001, China

[4]Key Laboratory of Ministry of Education for Conservation and Utilization of Special Biological Resources in the Western China, College of Life Science, Ningxia University, Yinchuan, 750021, China

*Correspondence to: Chao Wang, Email: wangcam@126.com; Tel.: +86 10 62733435; Center for Life Sciences, China Agricultural University, No.2 Yuan Ming Yuan West Road, Haidian District, Beijing, 100193, China.

#These authors contributed equally to this work.

*Corresponding authors.

Running title: SIRT1 regulates primordial follicle activation

Nonstandard Abbreviations

SIRT1	Sirtuin 1
PFs	primordial follicles
POI	premature ovarian insufficiency
PCOS	polycystic ovarian syndrome
IVA	*in vitro* activation
IVF	*in vitro* fertilization
dpc	days post coitum
dpp	days postpartum
pGCs	pregranulosa cells
RSV	resveratrol
PI3K	phosphatidylinositol 3-kinase
mTOR	mammalian target of rapamycin
Foxo3a	forkhead box o3a
PTEN	phosphatase and tensin homologue
TSC1/2	tumour suppressor tuberous sclerosis complex 1/2
mTORC1	mechanistic target of rapamycin complex 1
Kitl	Kit ligand
Foxl2	forkhead box l2
PMSG	pregnant mares serum gonadotropin
hCG	human chorionic gonadotropin
ITS	insulin-transferrin-selenium solution
FBS	fetal bovine serum

Abstract

In female mammals, the majority of primordial follicles (PFs) are physiologically quiescent, and only a few of them are activated and enter the growing follicle pool. Specific molecules, such as mTOR and AKT, have been proven to be important for PF activation. However, how the transcription of these genes is regulated is not clear. Although activators of mTOR or AKT have been successfully used to rescue the fertility of patients with premature ovarian insufficiency, the low efficacy and unclear safety profile of these drugs hinder their clinical use in the *in vitro* activation (IVA) of PFs.

Here, SIRT1, an NAD-dependent deacetylase, was demonstrated to activate mouse PFs independent of its deacetylase activity. SIRT1 was prominently expressed in pregranulosa cells and oocytes, and its expression was increased during PF activation. PF activation was achieved by either upregulating SIRT1 with a specific activator or overexpressing SIRT1. Moreover, SIRT1 knockdown in oocytes or pregranulosa cells could significantly suppress PF activation. Further studies demonstrated that SIRT1 enhanced both *Akt1* and *mTOR* expression by acting more as a transcription cofactor, directly binding to the respective gene promoters, than as a deacetylase. Importantly, we explored the potential clinical applications of targeting SIRT1 in IVA via short-term treatment of cultured ovaries from mice and human ovarian tissues to activate PFs by applying the SIRT1 activator resveratrol (RSV). RVA-induced IVA could be a candidate strategy to develop more efficient procedures for future clinical treatment of infertility.

Key words: Primordial follicle; SIRT1; *Akt1; mTOR; in vitro* activation; Resveratrol

Introduction

In females, follicles are the basic functional unit that supply mature oocytes throughout their reproductive life. Follicle development starts early in life when primordial follicles (PFs) are formed [1], and only a few dormant PFs are progressively recruited into the growing pool. Therefore, the rate of quiescent PF activation into immature oocytes is a critical process that determines the ovarian reserve and fertility life span. Disorders of initial PF recruitment lead to various ovarian diseases, including premature ovarian insufficiency (POI), which is diagnosed by amenorrhea before 40 years of age [2].

A PF consists of a meiotically arrested oocyte and flattened pregranulosa cells (pGCs). Previous studies have suggested that during the transformation of PF to primary follicles, cellular changes first occur in the pGCs and then in the oocyte [3]. In the past ten years, conditional gene knockout in mouse models have further shown that the initial recruitment of PFs is regulated by numerous signaling molecules. In oocytes, phosphatidylinositol 3-kinase (PI3K) and mammalian target of rapamycin (mTOR) signaling pathways play important roles in PF activation because conditional knockout of forkhead box o3a (Foxo3a), phosphatase and tensin homologue (PTEN), and tumor suppressor tuberous sclerosis complex 1/2 (TSC1/2) in oocytes triggers massive oocyte activation [4-12]. Based on a series of mouse models, Zhang et al. suggest that pGCs initiate PF activation and govern the development of dormant oocytes by triggering mechanistic target of rapamycin complex 1 (mTORC1)-Kit ligand (Kitl) signaling to activate the PI3K signaling pathway, which consequently activates dormant oocytes [13].

For POI patients, only limited number of individual successfully conceived despite undergoing diverse hormone therapies and ovulation induction treatments, including a full *in vitro* fertilization (IVF) cycle [14, 15]. Preovulatory follicles are a prerequisite for IVF; Unfortunately, POI patients have a relatively limited numbers of preovulatory follicles, although relatively rich resources of PFs are available in the ovaries. Thus, developing new methods for treating infertility by making good use of the patients'own PFs store will be favorable for such patients. In line with this, *in*

vitro activation (IVA) was invented and has become an indispensable technique for performing IVF in POI patients and cancer survivors via auto/allo-transplantation of activated PFs in ovarian tissues to produce mature oocytes during assisted reproduction procedures [16-22]. While the idea is promising, the present strategies for the IVA of PFs are quite inefficient, complex and costly. Patients must undergo two surgeries to accomplish one IVA cycle [18, 20]. Meanwhile, it is still uncertain whether there are potential negative effects of the drugs on oocyte quality [23, 24]. Therefore, the use of safer medicines, execution of less invasive procedures, easier recovery of oocytes and avoidance of complications related to prior pelvic surgery and adhesive disease are the key points to be resolved before the IVA technique can be widely used in the clinical setting.

Sirtuins could be potential targets for therapeutic applications in reproductive medicine [25]. Sirtuin 1 (SIRT1) is an NAD-dependent deacetylase that requires NAD^+ as a cofactor and functions by deacetylating intracellular targets, including transcription factors, signaling molecules and chromatin histones [26-29], all of which consequently play important roles in various pathophysiological processes such as cellular senescence/aging, apoptosis/proliferation and human longevity [30-32]. SIRT1 regulates the proliferation and apoptosis of ovarian granulosa cells [33]. Interestingly, it is also required in male germ cells for differentiation and fecundity in mice [34-36], suggesting that SIRT1 may participate in the regulation of germ cell development. Resveratrol (RSV), the natural polyphenolic compound activator of SIRT1 [37], promotes the activation of ovine PFs *in vitro* [38]. Therefore, given the multiple roles of SIRT1, it is likely a candidate drug for regulating early follicle development. However, the underlying function and mechanism of SIRT1 in PF activation is unclear.

In this study, we demonstrated that during PF initial recruitment, enriched SIRT1 expression in both pGCs and oocytes triggers the progressive activation of dormant PFs into growing follicles in mice. In pGCs, SIRT1 actively regulates the differentiation of pGCs into granulosa cells, while in dormant oocytes, SIRT1 triggers PTEN-PI3K-AKT signaling which then activates PFs. Interestingly, SIRT1 triggers

PF activation not through its deacetylase activity *in vitro* but rather as a transcription cofactor. We further demonstrated that RSV could be a candidate drug for IVA of human PFs.

Materials and Methods

Animal treatment and ovary collection

Adult female CD-1, C57BL/6J and NOD-SCID mice were purchased from Beijing Vital River Laboratory Animal Technology Co., Ltd. and bred to male mice of the same strain. CD-1 mice were used in all of the experiments except as otherwise noted. For experiments involving the *in vitro* activation of mouse PFs, female C57BL/6J mice were used as donors and recipients. NOD-SCID female mice were used as the recipients for experiments involving the *in vitro* activation of human PFs. For the *in vitro* fertilization experiments, C57BL/6J mice were used as sperm donors or superovulated mice. Mice were housed under controlled lighting (12 h light/12 h dark) and temperature (22-24°C) conditions and provided free access to food and water. Vaginal plug detection was considered 0.5 days post coitum (dpc), and the first 12 h after birth was considered 0 days postpartum (dpp). All procedures were conducted in accordance with the guidelines of and approved by the Animal Research Committee of the China Agricultural University, P. R. China. Human ovarian cortex fragments were obtained from patients with polycystic ovarian syndrome (PCOS). Informed consent from the patient and approval from the Human Subject Committee of Shandong University and China Agriculture University were obtained.

Chemicals and *in vitro* ovary organ culture

Unless otherwise specified, all chemicals and reagents used in the present study were purchased from R&D Systems, Minneapolis, MN, USA.

Mouse ovaries were cultured in 1.2 mL of DMEM/F12 media (Thermo Scientific, USA) in a 6-well culture plate (NEST Biotechnology, China) at 37°C in an incubator containing 5% CO_2 with saturated humidity. The medium was supplemented with penicillin and streptomycin to prevent bacterial contamination and was changed every other day. Ovaries were randomly assigned to each group. The SIRT1 activator (RSV) and inhibitor (EX527) were both from Selleck (China). They were used to treat

cultured 2 dpp ovaries from mice, which were further cultured for 2 or 3 days, while 1 dpp ovaries that had been transfected with either knockdown or overexpression vectors of *Sirt1* were cultured for 3 days or 4 days before examination.

Isolation of ovarian somatic cells and oocytes

2 dpp ovaries were cultured in the presence or absence of RSV for 2 days and then incubated in 100 μL 0.25% trypsin solution at 37°C for 5–10 min. Ovarian tissues were digested into single-cell suspensions, and the digestion reaction was terminated by 20% fetal bovine serum (FBS). The cell suspension was centrifuged at 3000 rpm for 5 min at 4°C, after which the supernatant was discarded, and the resulting pellet was resuspended in 1 mL phosphate-buffered saline (PBS). The cell suspension was then centrifuged at 4°C and 3000 rpm for 5 min, and the supernatant was discarded. Ovarian cells were resuspended in 500 μL DMEM/F12 supplemented with 5% FBS and 1% modified insulin-transferrin-selenium (ITS) solution (51500056, Life Technology, USA). The ovarian cell suspension was seeded into 24-well plates and cultured in the presence or absence of RSV at 37°C and 5% CO2 for 3-4 h. The plates were gently shaken to lift any loosely adherent oocytes, and the supernatants were collected for centrifugation to collect the oocyte components. The somatic cell component that adhered to the culture plate was recovered by digestion using 0.25% trypsin. Collected cells were washed in PBS for further examination.

Immunofluorescence and immunohistochemistry

Ovaries were fixed overnight in 4% paraformaldehyde, dehydrated through a graded series of ethanol, and then imbedded in paraffin. Embedded ovaries were sliced into sections 5 μm thick. For immunofluorescence, sections were deparaffinized and then rehydrated. After the sections were washed in PBS, they were boiled in a microwave for 16 min in citrate buffer (10 mM sodium citrate, 0.05% Tween 20, pH=6.0) for antigen retrieval. The sections were then blocked with 10% donkey serum followed by incubation with primary antibodies overnight at 4°C. Subsequently, the sections were incubated with Alexa Fluor 488- or Alexa Fluor

555-conjugated secondary antibodies (Thermo Scientific, USA) at room temperature for 60 min in PBS. Next, the sections were rinsed with PBS and stained with DAPI for 1 min. Finally, 20 μL Vectashield mounting medium (Applygen, China) was applied to each slide, and the sections were sealed with a coverslip. Immunohistochemistry was performed using Vectastain ABC kits and DAB peroxidase substrate kits (Vector Laboratories, Burlingame, CA, USA) according to the manufacturers' protocols. A Nikon 80i or Nikon A1 camera was used to image the immunofluorescent sections. An isotype-matched IgG was used as the negative control. The antibodies used and their application are listed in Table S1.

Histological sections and follicle counts

Ovaries were fixed in cold 4% paraformaldehyde for 24 h, embedded in paraffin, and serially sectioned at 5-μm (5 dpp ovaries) or 8-μm (adult ovaries) thickness. The sections were stained with hematoxylin, and the number of follicles per ovary was counted only when they contained oocytes with clearly visible nuclei. There were two types of follicles in the ovaries: PF (a single oocyte surrounded by several flattened pregranulosa cells) and growing follicle (an enlarged oocyte surround by a mixture of squamous and cuboidal somatic cells or an enlarged oocyte surrounded by one or several layers of cuboidal granulosa cells).

Ovarian follicles at different stages of development, including primordial (type 2), primary (type 3), secondary (type 4 and 5), and antral (type 6 and 7) follicles, were counted in all sections of an ovary based on the well-accepted standards established by Pedersen and Peters [39].

Real-time PCR analysis

Total RNA was isolated from ovaries with TRIzol reagent (Thermo Scientific, USA), and 1 μg of total RNA was used to synthesize cDNA according to the manufacturer's instructions (Thermo Scientific, USA). Real-time PCR using SYBR Green was performed on an ABI sequence detector system according to the manufacturer's protocol (Thermo Scientific, USA), and the expression of individual

genes was normalized to the levels of *β-actin*. Three samples from the indicated stages were collected, and reactions were performed at least 3 times for each sample. The primers used are listed in Tables S2 and S3.

Western blotting analysis

Ovaries were lysed with RIPA buffer (Cell Signaling, Danvers, MA, USA) containing 1 mM phenylmethylsulfonyl fluoride (Cell Signaling, Danvers, MA, USA). Protein concentrations in each group were determined using a bicinchoninic acid assay reagent (Beyotime Biotechnology, China) according to the manufacturer's recommendations. Equal amounts of protein per lane were separated by electrophoresis through a 10% SDS-polyacrylamide gel. Proteins were transferred onto PVDF membranes, and Western blotting was performed using the corresponding antibodies. The antibodies used are listed in Table S1.

RNA interference (RNAi) and gene overexpression

To ensure that the *Sirt1* knockdown and overexpression vectors would be transfected into the inner cells of mouse ovaries, every knockdown or overexpression vector was first injected into isolated 1 dpp mouse ovaries using glass pipettes under a stereomicroscope. After the ovaries were injected with the liquid, electrotransfection was performed by applying three 5-ms-long quasi-square pulses at a pulse-field strength of up to 30 V/cm. Both the *Sirt1* knockdown and cell-specific knockdown vectors were purchased from Thermo Scientific Inc., with the following knockdown sequence: AGTGAGACCAGTAGCACTAAT. The control shRNA vector contained a scrambled siRNA sequence that did not specifically target any known mouse mRNA sequences. The ovaries were then cultured for either 3 days to test the knockdown or overexpression efficiency at the mRNA and protein level or 4 days for histological examination and follicle counting.

Chromatin immunoprecipitation (ChIP)

ChIP assays were performed using a MAGNA ChIP kit (Merck, Germany)

according to the manufacturer's protocol. Immunoprecipitation was performed with crosslinked chromatin from 4 dpp mouse ovaries and either 8 μL anti-SIRT1 antibody or 1 μL normal mouse IgG (Merck, Germany). The enriched DNA was quantified by real-time PCR. The primers used are listed in Table S4.

Plasmid construction

To overexpress the *Sirt1* gene, wild-type *Sirt1* and the point mutant SIRT1-H355Y were cloned into pCMV-C-His (D2650, Beyotime, China). Golden Star T6 Super PCR mix was purchased from Beijing Tsingke Co., Ltd. All of the constructs were verified by sequencing. The primers used are listed in Tables S5 and S6.

***In vitro* activation of follicles and fresh tissue transplantation**

For mice, 35 dpp ovaries were cut into 4 pieces on average, while for humans, the ovarian cortex was isolated and cut into small cubes (≈1.5 mm^3) before incubation. The fragments or the whole ovaries from 5 dpp mice were first incubated with RSV for 30 min. Then, the ovaries were transferred into basal medium for an additional 12 h, and variations in PI3K and mTOR expression were detected.

To observe the effect of IVA on follicle development *in vivo*, ovaries were first treated with RSV for 30 min, transplanted under the kidney capsule of recipient mice, and allowed to develop for an additional 14 days. For the convenience of comparison, paired ovaries (treated and untreated) from the same donor were transplanted under separate sides of the kidney capsule in the same ovariectomized adult (8-week-old) recipient. All of the *in vitro* incubations were performed under standard culture conditions at 37°C in 5% CO_2 with saturated humidity.

***In vitro* fertilization**

One day after transplantation, mice transplanted with 5 dpp ovaries were treated daily with 2 IU pregnant mare serum gonadotropin (PMSG) (110044564, Ningbo Sansheng Pharmaceutial, China). Recipient mice were sacrificed at 14 or 18 days after

transplantation; the latter group was injected with 10 IU hCG (110041282, Ningbo Sansheng Pharmaceutial, China) and killed 14-16 h later to harvest MII oocytes. MII oocytes collected from superovulated mice served as a positive control. Sperm were incubated in HTF medium under mineral oil for 1 h. Sperm ($1\text{-}5\times10^5$) were added to 100 μL HTF medium containing MII oocytes for 6 h, after which any inseminated oocytes were removed into 50 μL droplets of KSOM media (MR-020P-5F, Millipore, USA) under mineral oil and incubated for 96 h. All of the incubations were performed under standard culture conditions at 37°C in 5% CO_2 with saturated humidity.

Statistical analysis

All experiments were repeated at least three times, and the values are presented as the means ± SEM. The data were analyzed by t test or ANOVA, and differences were considered statistically significant at $P < 0.05$.

Results

Spatiotemporal expression of SIRT1 correlates with follicular initial recruitment

To clarify the expression pattern of SIRT1 in the ovaries of newborn mice, immunohistochemistry assays were performed and showed that SIRT1 was expressed in the nuclei of both pGCs and oocytes (Fig. 1A). In addition, reverse transcription real-time PCR (RT-qPCR) and Western blotting analyses demonstrated that the mRNA and protein levels of *Sirt1* were both elevated from 5 dpp to 7 dpp compared to the levels in 3 dpp ovaries (Fig. 1B and 1C). Therefore, elevated SIRT1 expression in the newborn mouse ovaries was closely related to the initiation of PF recruitment.

Subsequently, to investigate the function of SIRT1 during PF activation, an *in vitro* ovary culture system was employed. Based on this model, either RSV (a specific activator of SIRT1) or a CMV-driven *Sirt1*-overexpression (*Sirt1*-OE) vector was introduced into cultured ovaries. Briefly, either 2 dpp mouse ovaries were cultured with RSV (40 μM) for 1-3 days or 1 dpp ovaries were injected with a *Sirt1*-OE vector and cultured for 3-4 days. Importantly, as the level of SIRT1 was elevated, ovarian growth was accelerated (Fig. S1 A-C), and significantly more growing follicles were found in the treatment groups than in the respective control groups. The whole-ovary quantitative data further supported the findings (Fig. 1D-G and Fig. S1 D-E). These results confirmed the speculation that SIRT1 enrichment in both pGCs and oocytes

participates in the initial recruitment of PFs.

SIRT1 activates PF development independent of its deacetylase activity

To further verify the regulatory role of SIRT1 in initial follicular recruitment, we used EX527, an inhibitor of SIRT1 (Fig. S2), to specifically block its deacetylase activity *in vitro*. Unexpectedly, when 2 dpp ovaries were cultured with EX527 (1.5 μM) for 3 days, the number of growing follicles was significantly greater than that in the control condition (Fig. 2A and 2B), suggesting that EX527 stimulated PF development. To validate the efficacy of EX527, we treated 2 dpp mouse ovaries with EX527 for 2 days and then analyzed total ovarian protein content via Western blotting. EX527 treatment not only increased the acetylation level of H3K9 (H3K9ac), the direct deacetylation site of SIRT1, but also sharply increased SIRT1 expression (Fig. 2C). Collectively, we hypothesized that when EX527 weakened SIRT1 deacetylase activity, the ovary generates a negative feedback loop to upregulate SIRT1, and when SIRT1 was upregulated, it promoted PF activation. In other words, SIRT1 activated PF development by augmenting SIRT1 expression instead of promoting its deacetylase activity.

To further confirm this hypothesis, a *Sirt1* knockdown vector (*Sirt1*-KD) and a catalytically inactive mutant vector (SIRT1-H355Y) were constructed, which were injected into 1 dpp ovaries and then cultured for an additional 4 days. There were notably fewer activated follicles when either of these vectors was injected than the number observed in the control condition after RNA interference (RNAi) (Fig. 2D and 2E). In contrast, the number of growing follicles increased significantly after SIRT1-H355Y overexpression (Fig. 2G and 2H). In line with the decrease in SIRT1 after RNAi, a significant increase in H3K9ac was also detected (Fig. 2F), probably as a consequence of the lack of deacetylase activity in these ovaries after gene silencing. Alternatively, overexpression of the mutant SIRT1 plasmid resulted in no deacetylase activity, and the level of H3K9ac was not changed, although the level of mutated SIRT1 was significantly high (Fig. 2I). These results confirm the hypothesis that the activation of PFs is regulated by modifying SIRT1 expression.

Taken together, these results suggest that SIRT1 participates in PF activation independent of its deacetylase activity.

SIRT1 triggers PF awakening by activating the PTEN-PI3K-AKT and TSC1/2-mTOR signaling pathways

To uncover the mechanism by which SIRT1 affects PF activation, the response of two classical pathways, namely, the PTEN-PI3K-AKT and TSC1/2-mTOR signaling pathways (which have been proven to be pivotal for PF activation), were studied, as shown below.

Western blotting analyses showed that treatment with RSV or EX527 and overexpression of the mutant SIRT1-H355Y significantly elevated the level of SIRT1 in mouse ovaries compared to that in the control (Fig. 3A and 3B). With the upregulation of SIRT1, the levels of phosphorylated and total AKT and mTOR proteins were increased, whereas the levels of PTEN and TSC1 were decreased (Fig. 3A, 3B and S3A-S3D). AKT-dependent phosphorylation of Foxo3a promotes its export from the nucleus to the cytoplasm when PI3K signaling is activated in oocytes. Our results showed that p-Foxo3a was increased after treatment with RSV or EX527 or overexpression of the mutant SIRT1-H355Y (Fig. 3C-3E). Foxo3a translocation to the cytoplasm was significantly induced in primordial oocytes of the cortex region in RSV- and EX527-treated ovaries compared with that in the control. Whole-ovary quantitative data for Foxo3a in the nucleus and cytoplasm further supported the findings (Fig. 3F, 3G, S3E and S3F), indicating that the PI3K signaling pathway was soundly activated. To further verify the regulatory role of SIRT1 in the function of key proteins, *Sirt1* knockdown was performed, which led to a reduction in the expression of mTOR and AKT both at the phosphorylated and total protein levels and a decrease in the expression of p-Foxo3a (Fig. 3H). This change was opposite to the effect of SIRT1 activation assays. These results suggested that SIRT1 regulated the PTEN-PI3K-AKT and TSC1/2-mTOR signaling pathways.

To explore how the key proteins were regulated, we performed RT-qPCR analyses and the results showed that RSV, EX527 and *Sirt1*-OE treatments changed the expression of these genes, including *mTOR*, *Akt1*, *Tsc1*, *Kit* and *Kitl*, at the transcriptional level (Fig. 3H and S3G). *Sirt1* knockdown was also performed, and the expression of these genes at the transcriptional level was opposite the expression observed in the SIRT1 activation assays. (Fig. 3J). These results suggest that SIRT1 regulates the transcription of related genes.

In summary, these findings confirmed that both the PTEN-PI3K-AKT-Foxo3a and TSC1/2-mTOR signaling pathways within the mouse ovary were activated with

the increased levels of SIRT1, thereby facilitating PF activation.

SIRT1 in granulosa cells and oocytes synergistically regulates primordial follicular activation

To determine the effects of SIRT1 in pGCs and oocytes on PF activation, an assay specifically silencing *Sirt1* in either pGCs or oocytes was performed. Following procedures resembling those of systematic RNAi treatment in the whole ovary, a cell-type-specific knockdown vector with a GFP tag was constructed (Fig. S4A). First, immunofluorescence staining indicated that both knockdown vectors worked well in our *in vitro* culture system, in which GFP expression was driven by either the *Foxl2* promoter in pGCs or the *Gdf9* promoter in oocytes (Fig. 4A). Second, after 1 dpp mouse ovaries were injected with either the *Foxl2-Sirt1*-shRNA or *Gdf9-Sirt1*-shRNA vectors and cultured for 4 days, the ovaries in both treatment groups exhibited significantly less follicular activation in the cortical regions than did the ovaries in the respective control groups (Fig. 4B and S4B). This result implied that SIRT1 expressed in pGCs and oocytes is involved in the activation of PFs.

To elucidate which signaling pathways are regulated by SIRT1 in granulosa cells and oocytes, we performed RT-qPCR after the cell-type-specific plasmids were transfected into mouse ovaries. The results showed that *Foxl2*-driven *Sirt1* knockdown led to a significant decrease in *mTOR* and *Kitl* expression and an increase in *Tsc1* expression in pGCs, while *Gdf9*-driven *Sirt1* knockdown caused a decrease in *mTOR*, *Akt1*, and *Kit* expression and an increase in *Pten* expression in oocytes (Fig. 4C). These results suggested that SIRT1 regulates PF activation via the mTOR signaling pathway in pGCs, whereas SIRT1 affects oocyte growth by activating the PI3K and mTOR signaling pathways.

To further confirm the synergistic regulation of SIRT1 in granulosa cells and oocytes, 2 dpp ovaries were cultured for 2 days in the presence or absence of RSV, and somatic cells and oocytes were isolated to detect changes in related molecules. The results showed that the isolation of somatic cells and oocytes was feasible (Fig. S5). The transcription of *Akt1* and *Kit* was increased while that of *Pten* was decreased in oocytes with upregulated *Sirt1* expression. By contrast, the transcription of *mTOR* and *Kitl* was increased and that of *Tsc1* was decreased in granulosa cells with upregulated *Sirt1* expression; *Akt1* expression was not changed in granulosa cells with upregulated *Sirt1* (Fig. 4D). This finding suggested that SIRT1 enhanced the

transcription of *mTOR* in granulosa cells, which produce more Kitl; Kitl activates the PI3K pathway in oocytes by binding to Kit, leading to nuclear exclusion of Foxo3a and activation of PFs. Meanwhile, SIRT1 also enhanced the transcription of *mTOR* and *Akt1* in oocytes and the activation of dormant oocytes. Therefore, SIRT1 promoted both pGC and oocyte development.

SIRT1 directly binds to the respective promoters of *Akt1* and *mTOR*

Next, we investigated whether SIRT1 governs PF activation by directly binding to the promoters of *Akt1*, *mTOR*, *Pten* or *Tsc1* to regulate their transcription. First, freshly collected 4 dpp mouse ovaries were used to perform chromatin immunoprecipitation (ChIP)-qPCR. The DNA fragments that immunoprecipitated with the anti-SIRT1 antibody were amplified with approximately 10 pairs of primers targeting the regions within 2000 bp of the promoter sequences of *Akt1*, *mTOR*, *Pten* or *Tsc1*. The results indicated strong binding of SIRT1 to the promoter regions of both *Akt1* and *mTOR* (-486 to -641 bp and -435 to -563 bp from the start of transcription, respectively) (Fig. 5A and 5B). In contrast, SIRT1 binding to the promoter regions of *Pten* and *Tsc1* was weak without exception (Fig. 5C). The results suggested that SIRT1 bound to the *Akt1* and *mTOR* promoters, which consequently modulated the transcription of the *Akt1* and *mTOR* genes.

Transient resveratrol treatment leads to IVA of mouse and human PFs

To clarify the potential usage of RSV in the IVA of mice and humans, serial studies were designed. First, RSV was applied for IVA in 5 dpp and 35 dpp mouse ovaries. Western blotting results showed that the transient RSV treatment significantly increased the levels of total and phosphorylated AKT and mTOR protein in each assay; these increases were also accompanied by elevated SIRT1 protein levels accordingly (Fig. 6A and 6B). Meanwhile, 5 dpp and 35 dpp mouse ovaries displayed greater nucleocytoplasmic transport of Foxo3a in PFs after RSV treatment than did ovaries from in the respective control groups (Fig. 6C, 6D, S5A and S5B). Taken together, these results suggest that transient RSV treatment simultaneously activated the PI3K and mTOR signaling pathways in cultured mouse ovaries.

To further verify the developmental capacity of the presumably activated mouse ovaries after RSV treatment, ovaries were transplanted under the kidney capsule of ovariectomized adult recipient mice (8 weeks old) and monitored for 14 days. In the

cortical region of the 5 dpp and 35 dpp ovaries, numerous activated follicles were observed in the RSV treatment group in contrast to the fewer PFs available in the respective control groups (Fig. 6E, 6F, S5C and S5D). The size and weight of the 5 dpp ovaries increased significantly in the RSV-treated groups compared with the paired controls after 14 days in response to a daily injection of 2 IU PMSG (Fig. 6G and 6H). Meanwhile, ovarian histology analysis and follicular count revealed the presence of antral follicles in RSV-treated ovaries but not in ovaries from the control groups (Fig. 6I and S5E). These results suggested that transient RSV treatment accelerated follicular development *in vitro*.

To prove the maturity and the developmental capacity of oocytes obtained from RSV-activated PFs, oocytes at the MII stage of meiosis collected from the RSV-treated ovaries after hCG injection were processed for IVF and early embryonic culture *in vitro*. MII oocytes collected from normal superovulating wild-type mice served as a positive control. The results showed that more MII oocytes were collected from the RSV-treated ovaries than from the ovaries that did not receive RSV treatment, while RSV-treated ovaries successfully fertilized oocytes from RSV-activated follicles could develop into blastocysts (Fig. 6J). The IVF ratios and early embryonic development were not significantly different from those in oocytes harvested with traditional IVF methods (Fig. 6K). The results suggested that transient RSV treatment could activate PFs *in vitro* without causing any side effects on mouse oocyte quality.

Next, we studied whether RSV can be applied to the IVA of human PFs. To confirm whether the cellular localization of SIRT1 during the early follicular development of human ovaries was similar to that of mice, an immunostaining assay was first performed. The results showed that SIRT1 was also expressed in the nuclei of both pGCs and oocytes (Fig. 7A). Western blotting showed that transient RSV treatment significantly activated both AKT and mTOR protein expression in treated human ovarian tissues (Fig. 7B and 7C). The *in vivo* transplantation assay showed that the number of activated PFs within RSV-treated ovarian tissue pieces was increased at 14 days after transplantation (Fig. 7D and Table S1). The results suggest that transient RSV treatment was also effective for the IVA of human PFs *in vitro*.

Collectively, these results demonstrated that SIRT1 facilitates PF recruitment by directly modulating *mTOR* and *Akt1* transcription and that transient RSV treatment was able to induce PF growth *in vitro*. Thus, RSV could be a potential drug for

performing IVA treatment in eligible patients (Fig. 8).

Discussion

The IVA technique represents a paradigm shift in fertility care [22]. The study of initial PF recruitment could help in the development of more effective IVA candidate drugs. Here, SIRT1 was shown to be pivotal in regulating the levels of key PI3K and mTOR signaling proteins simultaneously within a PF during the initial recruitment phase. Interestingly, SIRT1-induced activation of PFs does not depend on its deacetylase activity but rather on its function as a transcription cofactor in modulating the expression levels of genes related to classical PF activation. More importantly, as one of the activators of SIRT1, RSV is a promising candidate drug that can efficiently activate the PFs of mice and humans *in vitro*, which may contribute to reducing surgical procedures required and the costs of IVA.

According to the most recent studies, pGCs initiate PF activation and govern the development of dormant oocytes by triggering mTORC1-Kitl signaling inside somatic cells. After Kitl binds to its receptor on the oocyte membrane, it activates the PI3K signaling pathway to stimulate dormant oocytes [11]. Regarding mTOR, which is systematically expressed in oocytes and granulosa cells [6-8, 11, 42], serial studies have demonstrated its indispensable roles in regulating PF activation. Interestingly, mTOR expression in pGCs triggers follicular activation through Kitl-Kit signaling [11], whereas our study showed that overactivation of mTOR signaling in the oocytes of PFs leads to a global activation of the follicular pool. Impressively, SIRT1 regulates the transcription of *Akt1* and mTOR simultaneously and then accelerates PF activation. This finding contributes to a deeper understanding of the process of PF activation.

As a member of the NAD^+-dependent class III histone deacetylases, SIRT1 plays diverse physiological roles as an enzyme and a repressor of gene transcription. However, cumulative evidence has indicated that SIRT1 is also involved in assisting gene transcription independent of its enzymatic activity [43-45]. For instance, SIRT1 enhances the transcription of the glucocorticoid receptor (GR) in a deacetylase

activity-independent fashion [45]. In agreement with these findings, our study also provided evidence demonstrating that SIRT1 activates dormant PF development independent of its deacetylase activity but rather acts as a transcription cofactor that assists the expression of multiple genes related to PF activation. Collectively, these data indicate that SIRT1 actively takes part in the activation of PFs more as a general indirect gene transcription enhancer than as a specific enzyme.

The functions of SIRT1 in the ovaries of rodents seem to be completely different depending on how the ovaries were treated, including the concentration of SIRT1 used and whether the ovaries were treated *in vitro* or *in vivo* [46-49]. Here, after applying different activators and upregulated/downregulated expression systems of SIRT1, we have proven that SIRT1 is actively and highly efficiently involved in the activation of PFs *in vitro*, in which mTOR and AKT were upregulated. Our results are consistent with previous reports of successful IVA treatments in mice and humans [16, 18-20, 50]. Interestingly, a series of *in vivo* studies in rodents stated that activated SIRT1 contributes to preserving age-related reproduction potential [46-49]. They found that in aging mice treated with RSV, in fat mice treated with SRT1720, and even in ZP3-drivern transgenic *Sirt1* mice, the reproductive span was longer than that in the respective control mice. Regarding the possible mechanism for this extension of reproductive function, Luo et al. believe that the downregulation of mTOR and activation of Foxo3a within ovaries may be the key point for the preservation of mouse fertility by increasing PF numbers [47, 49]. However, the authors did not provide direct evidence demonstrating that SIRT1 prevents PF activation. Coincidentally, Su et al. proved that conditional knockout of *mTOR* in nongrowing primordial oocytes results in defective follicular development leading to the progressive degeneration of oocytes and granulosa cell transdifferentiation [42]. Collectively, much work is needed before one can clearly explain the time- and dose-dependent actions of SIRT1 in various conditions.

The IVA approach has opened a new window for POI and cancer patients who desire to conceive their own genetic children; however, it has also aroused concerns regarding its efficacy and safety. The existing IVA strategy requires *in vitro* incubation

of ovarian tissue for longer than 24 h. An adverse effect of this treatment is that the patients have to undergo two laparoscopic surgeries, which not only can increase complications in patients but is costly and time consuming. In addition, the potential negative effects of the drugs on the quality of oocytes raise major concerns [22]. Fortunately, our recently published data showed that activating oocyte-specific cell division cycle 42 (CDC42) positively influences the IVA procedure with highly efficient outputs in mice, which reduces the incubation time to 30 min [50]. Coincidentally, we have proven that the IVA procedures for the treatment of ovarian tissue in mice as well as in humans can be reduced to 30 min by administering RSV. Last but not least, our results showed that oocytes from RSV-treated ovaries could successfully develop into blastula, which is in line with reports stating that RSV improves the *in vitro* maturation of oocytes and enhances oocyte quality in aged mice and humans [46, 51]. In conclusion, the application of RSV in the clinic could be a more efficient and attractive strategy of IVA.

In summary, we have reported that global activation of SIRT1 in pGCs and oocytes initiates the progression of PF activation in the mammalian ovary under *in vitro* conditions. The results presented here provide a better understanding of ovarian physiology and pathology. In addition, applying RSV during the IVA procedure could make the technique safer, cheaper and more promising in clinical practice.

Acknowledgements

The authors wish to thank each member of Xia Lab for their valuable discussion and Nature Research Editing Service for language revision. This study was supported by grants from the National Key Research & Developmental Program of China grant number 2017YFC1001100 to G.X.; the National Basic Research Program of China grant numbers 2014CB943202 to C.W.; 2013CB945501 to G.X., 2014CB138503 to B.Z.; the National Natural Science Foundation of China grant numbers 31872792 to C.W.; 31371448, 31571540 to G.X.; the Beijing Natural Science Foundation grant numbers 5182015 to C.W., 7182090 to G.X.; Project of State Key Laboratory of Agrobiotechnology grant numbers 2015SKLAB4-1 to C.W., 2016SKLAB-1 to G. X.

and Institution of Higher Education Projects of Building First-class Discipline Construction in Ningxia Region (Biology) grant number NXYLXK2017B05 to G. X.. The authors declare no conflicts of interest.

Author contributions

Zhang T, Du X, and Zhao L. performed most of the experiments and wrote the manuscript. He M, Lin L, Guo C, Zhang X, Han J, Huang K, Sun G, Yan H, Yan Lei and Zhou B performed part of the experiment. Qin Y provided human ovarian fragments. Wang C and Xia G supervised the whole project and wrote the manuscript. All authors read and approved the final manuscript.

References

1 Wang, C., Zhou, B., Xia, G. (2017) Mechanisms controlling germline cyst breakdown and primordial follicle formation. *Cell. Mol. Life Sci.* 74(14):2547-2566.

2 Qin, Y., Jiao, X., Simpson, JL., Chen, ZJ. (2015) Genetics of primary ovarian insufficiency: new developments and opportunities. *Hum. Reprod. Update* 21(6):787-808.

3 Hirshfield, AN. (1991) Development of follicles in the mammalian ovary. *Int. Rev. Cytol.* 124:43-101.

4 Liu, K., Rajareddy, S., Liu, L., Jagarlamudi, K., Boman, K., Selstam, G., Reddy, P. (2006) Control of mammalian oocyte growth and early follicular development by the oocyte PI3 kinase pathway: new roles for an old timer. *Dev. Biol.* 299(1):1-11.

5 Reddy, P., Adhikari, D., Zheng, W., Liang, S., Hämäläinen, T., Tohonen, V., Ogawa, W., Noda, T., Volarevic, S., Huhtaniemi, I., Tohonen, V., Ogawa, W., Noda, T., Volarevic, S., Huhtaniemi, I., Liu, K. (2009). Pdk1 signaling in oocytes controls reproductive aging and lifespan by manipulating the survival of primordial follicles. *Hum. Mol. Genet.* 18(15):2813.

6 Adhikari, D., Zheng, W., Shen, Y., Gorre, N., Hämäläinen, T., Cooney, A. J., Huhtaniemi, I., Lan, Z. J., Liu, K. (2010) Tsc/mTORC1 signaling in oocytes governs the quiescence and activation of primordial follicles. *Hum. Mol. Genet.* 19(3):397-410.

7 Gorre, N., Adhikari, D., Lindkvist, R., Brännström, M., Liu, K., Shen, Y. (2014) mTORC1 signaling in oocytes is dispensable for the survival of primordial follicles and for female fertility. *PloS One* 9(10):e110491.

8 Adhikari, D., Flohr, G., Gorre, N., Shen, Y., Yang, H., Lundin, E., Lan, ZJ., Gambello, MJ., Liu, K. (2009) Disruption of tsc2 in oocytes leads to overactivation of the entire pool of primordial follicles. *Mol. Hum. Reprod.* 15(12):765-70.

9 Castrillon, D. H., Miao, L., Kollipara, R., Horner, J. W., Depinho, R. A. (2003) Suppression of ovarian follicle activation in mice by the transcription factor foxo3a. *Science* 301(5630):215-218.

10 Reddy, P., Liu, L., Adhikari, D., Jagarlamudi, K., Rajareddy, S., Shen, Y., Du, C., Tang, W., Hämäläinen, T., Peng, S., Lan, ZJ., Cooney, AJ., Huhtaniemi, I., Liu, K. (2008) Oocyte-specific deletion of pten causes premature activation of the primordial follicle pool. *Science* 319(5863):611-613.

11 Zhang, H., Risal, S., Gorre, N., Busayavalasa, K., Li, X., Shen, Y., Bosbach, B., Brännström, M., Liu, K. (2014) Somatic cells initiate primordial follicle activation and govern the development of dormant oocytes in mice. *Curr. Biol.* 24(21):2501.

12 Adhikari D, Liu K (2009) Molecular mechanisms underlying the activation of mammalian primordial follicles. Endocr. Rev. 30(5):438-464.

13 Zhang, H., Liu, K. (2015) Cellular and molecular regulation of the activation of mammalian primordial follicles: somatic cells initiate follicle activation in adulthood. *Hum. Reprod. Update* 21(6):779-86.

14 Bidet, M., Bachelot, A., Bissauge, E., Golmard, JL., Gricourt, S., Dulon, J., Coussieu, C., Badachi, Y., Touraine, P. (2011) Resumption of ovarian function and pregnancies in 358 patients with premature ovarian failure. *J. Clin. Endocrinol. Metab*. 96(12):3864.

15 Wang, X., Gook, D. A., Walters, K. A., Anazodo, A., Ledger, W. L., Gilchrist, R. B. (2016) Improving fertility preservation for girls and women by coupling oocyte *in vitro* maturation with existing strategies. *Womens Health* 12(3):275-278.

16 Li, J., Kawamura, K., Cheng, Y., Liu, S., Klein, C., Liu, S., Duan, E., Hsueh, AJ. (2010) Activation of dormant ovarian follicles to generate mature eggs. *Proc. Natl . Acad. Sci. U. S. A.* 107(22):10280-10284.

17 Adhikari, D., Gorre, N., Risal, S., Zhao, Z., Zhang, H., Shen, Y., Liu, K. (2012) The safe use of a pten inhibitor for the activation of dormant mouse primordial follicles and generation of fertilizable eggs. *PloS One* 7(6):e39034.

18 Kawamura, K., Cheng, Y., Suzuki, N., Deguchi, M., Sato, Y., Takae, S., Ho, CH., Kawamura, N., Tamura, M., Hashimoto, S., Sugishita, Y., Morimoto, Y., Hosoi, Y., Yoshioka, N., Ishizuka, B., Hsueh, AJ. (2013) Hippo signaling disruption and Akt stimulation of ovarian follicles for infertility treatment. *Proc. Natl . Acad. Sci. U. S. A.* 110(43):17474-9.

659 19 Sun, X., Su, Y., He, Y., Zhang, J., Liu, W., Zhang, H., Hou, Z., Liu, J., Li, J. (2015)
660 New strategy for *in vitro* activation of primordial follicles with mTOR and PI3K
661 stimulators. *Cell Cycle* 14(5):721-731.
662 20 Zhai, J., Yao, G., Dong, F., Bu, Z., Cheng, Y., Sato, Y., Hu, L., Zhang, Y., Wang, J.,
663 Dai, S., Li, J., Sun, J., Hsueh, AJ., Kawamura, K., Sun, Y. (2016) *In vitro* activation
664 of follicles and fresh tissue auto-transplantation in primary ovarian insufficiency
665 patients. *J. Clin. Endocrinol. Metab.* 101(11):4405-4412.
666 21 Kawamura, K., Kawamura, N., Hsueh, AJ. (2016) Activation of dormant follicles:
667 a new treatment for premature ovarian failure?. *Curr. Opin. Obstet. Gynecol.*
668 28(3):217-222.
669 22 Yin, O., Cayton, K., Segars, J. H. (2016) *In vitro* activation: a dip into the
670 primordial follicle pool?. *J. Clin. Endocrinol. Metab.* 101(10):3568.
671 23 Cordeiro, CN., Christianson, MS., Selter, JH., Segars, JH Jr. (2016) *In vitro*
672 activation a possible new frontier for treatment of primary ovarian insufficiency.
673 *Reprod. Sc*i. 23(4):429-438.
674 24 Ladanyi, C., Mor, A., Christianson, M. S., Dhillon, N., Segars, J. H. (2017) Recent
675 advances in the field of ovarian tissue cryopreservation and opportunities for
676 research. *J. Assist. Reprod. Genet.* 34(6):709-722.
677 25 Tatone, C., Di, G. E., Barbonetti, A., Carta, G., Luciano, A. M., Falone, S.,
678 Amicarelli, F. (2018) Sirtuins in gamete biology and reproductive physiology:
679 emerging roles and therapeutic potential in female and male infertility. *Hum.*
680 *Reprod. Update* 24(3):267-289.
681 26 Brunet, A., Sweeney, L. B., Sturgill, J. F., Chua, K. F., Greer, P. L., Lin, Y., Tran,
682 H., Ross, S. E.,Mostoslavsky, R., Cohen, HY., Hu, LS., Cheng, HL, Jedrychowski,
683 MP., Gygi, SP., Sinclair, DA., Alt, FW., Greenberg, ME. (2004) Stress-dependent
684 regulation of foxo transcription factors by the sirt1 deacetylase. *Science*
685 303(5666):2011-2015.
686 27 Sundaresan, NR., Pillai, VB., Wolfgeher, D., Samant, S., Vasudevan, P., Parekh, V.,
687 Raghuraman, H., Cunningham, JM., Gupta, M., Gupta, MP. (2011) The deacetylase
688 sirt1 promotes membrane localization and activation of Akt and Pdk1 during

689 tumorigenesis and cardiac hypertrophy. *Sci. Signaling* 4(182):46.
690 28 Vaquero, A., Scher, M., Lee, D., Erdjument-Bromage, H., Tempst, P., Reinberg, D.
691 (2004) Human sirt1 interacts with histone H1 and promotes formation of
692 facultative heterochromatin. *Mol. Cell* 16(1):93.
693 29 Vaquero, A., Sternglanz, R., Reinberg, D. (2007) NAD^+-dependent deacetylation
694 of H4 lysine 16 by class III HDACs. *Oncogene* 26(37):5505-5520.
695 30 Chung, S., Yao, H., Caito, S., Hwang, J. W., Arunachalam, G., Rahman, I. (2010)
696 Regulation of sirt1 in cellular functions: role of polyphenols. *Arch. Biochem.*
697 *Biophys.* 501(1):79-90.
698 31 Zhang, J., Lee, SM., Shannon, S., Gao, B., Chen, W., Chen, A., Divekar, R.,
699 McBurney, MW., Braley-Mullen, H., Zaghouani, H., Fang, D. (2009) The type III
700 histone deacetylase sirt1 is essential for maintenance of T cell tolerance in mice. *J.*
701 *Clin. Invest.* 119(10):3048.
702 32 Leibiger, I. B., Berggren, P. O. (2006) Sirt1: a metabolic master switch that
703 modulates lifespan. *Nat. Med.* 12(1):34.
704 33 Zhang, M., Zhang, Q., Hu, Y., Xu, L., Jiang, Y., Zhang, C., Ding, L., Jiang, R., Sun,
705 J., Sun, H.,Yan, G. (2017) Mir-181a increases foxo1 acetylation and promotes
706 granulosa cell apoptosis via sirt1 downregulation. *Cell Death Dis.* 8(10):3088.
707 34 Seifert, E. L., Caron, A. Z., Morin, K., Coulombe, J., He, X. H., Jardine, K., Darch,
708 D. D., Boekelheide, K., Harper, M. E., McBurney, M. W. (2012) Sirt1 catalytic
709 activity is required for male fertility and metabolic homeostasis in mice. *FASEB J*.
710 26(2):555-66.
711 35 Bell, EL., Nagamori, I., Williams, EO., Del, Rosario, AM., Bryson, BD., Watson,
712 N., White, FM., Sassone-Corsi, P., Guarente, L. (2014) Sirt1 is required in the male
713 germ cell for differentiation and fecundity in mice. *Development*
714 141(18):3495-3504.
715 36 Liu, C., Song, Z., Wang, L., Yu, H., Liu, W., Shang, Y., Xu, Z., Zhao, H., Gao, F.,
716 Wen, J., Zhao, L., Gui, Y., Jiao, J., Gao, F., Li, W. (2016) Sirt1 regulates acrosome
717 biogenesis by modulating autophagic flux during spermiogenesis in mice.
718 *Development* 144(3):441-451.

719 37 Cao, D., Wang, M., Qiu, X., Liu, D., Jiang, H., Yang, N., Xu, R. M. (2015)
720 Structural basis for allosteric, substrate-dependent stimulation of sirt1 activity by
721 resveratrol. *Genes Dev.* 29(12):1316-25.
722 38 Bezerra, MÉS., Gouveia, BB., Barberino, RS., Menezes, VG., Macedo, TJS.,
723 Cavalcante, AYP., Monte, APO., Santos, JMS., Matos, MHT. (2018) Resveratrol
724 promotes in vitro activation of ovine primordial follicles by reducing DNA damage
725 and enhancing granulosa cell proliferation via PI3 kinase pathway. *Reprod. Domest.*
726 *Anim.* 53:1298-1305.
727 39 Pedersen, T. (1970) Determination of follicle growth rate in the ovary of the
728 immature mouse. *J. Reprod. Fertil.* 21(1):81-93
729 39 Schmidt, D., Ovitt, C. E., Anlag, K., Fehsenfeld, S., Gredsted, L., Treier, A. C.,
730 Treier, M. (2004) The murine winged-helix transcription factor foxl2 is required for
731 granulosa cell differentiation and ovary maintenance. *Development*
732 131(4):933-942.
733 40 Uda, M., Ottolenghi, C. L., Garcia, J. E., Deiana, M., Kimber, W., Forabosco, A.,
734 Forabosco, A., Cao, A., Schlessinger, D., Pilia, G. (2004) Foxl2 disruption causes
735 mouse ovarian failure by pervasive blockage of follicle development. *Hum. Mol.*
736 *Genet.* 13(11):1171-1181.
737 41 Rajareddy, S., Reddy, P., Du, C., Liu, L., Jagarlamudi, K., Tang, W., Shen, Y.,
738 Berthet, C., Peng, SL., Kaldis, P., Liu, K. (2007) P27kip1 (cyclin-dependent kinase
739 inhibitor 1b) controls ovarian development by suppressing follicle endowment and
740 activation and promoting follicle atresia in mice. *Mol. Endocrinol.*
741 21(9):2189-2202.
742 42 Guo, J., Zhang, T., Guo, Y., Sun, T., Li, H., Zhang, X., Yin, H., Cao, G., Yin, Y.,
743 Wang, H., Shi, L., Guo, X., Sha, J., Eppig, JJ., Su, YQ. (2018) Oocyte
744 stage-specific effects of mTOR determine granulosa cell fate and oocyte quality in
745 mice. *Proc. Natl. Acad. Sci. U. S. A.* 115:5326-5333.
746 43 Nemoto. S., Fergusson, M. M., Finkel, T. (2015) Sirt1 functionally interacts with
747 the metabolic regulator and transcriptional coactivator pgc-1α. *J. Biol. Chem.*
748 280(16):16456-16460.

44 Pfister, J. A., Ma, C., Morrison, B. E., D'Mello, S. R. (2008) Opposing effects of sirtuins on neuronal survival: sirt1-mediated neuroprotection is independent of its deacetylase activity. *PloS One* 3(12):4090.

45 Suzuki, S., Iben, J. R., Coon, S. L., Kino, T. (2017) Sirt1 is a transcriptional enhancer of the glucocorticoid receptor acting independently to its deacetylase activity. *Mol. Cell. Endocrinol.* 461:178-187.

46 Liu, M., Yin, Y., Ye, X., Zeng, M., Zhao, Q., Keefe, D.L, Liu, L. (2013) Resveratrol protects against age-associated infertility in mice. *Hum. Reprod.* 28(3):707.

47 Zhou. XL., Xu, JJ., Ni, YH., Chen, XC., Zhang, HX., Zhang, XM., Liu, WJ., Luo, LL., Fu, YC. (2014) Sirt1 activator (SRT1720) improves the follicle reserve and prolongs the ovarian lifespan of diet-induced obesity in female mice via activating sirt1 and suppressing mTOR signaling. *J. Ovarian Res.* 7(1):1-12.

48 Liu, W., Zhang, X., Wang, N., Zhou, XL., Fu, YC., Luo, LL. (2015) Calorie restriction inhibits ovarian follicle development and follicle loss through activating SIRT1 signaling in mice. *Eur. J. Med. Res.* 20(1):22-22.

49 Long, GY., Yang, JY., Xu, JJ., Ni, YH., Zhou, XL., Ma, JY., Fu, YC., Luo, LL. (2019) SIRT1 knock-in mice preserve ovarian reserve resembling caloric restriction. *Gene* 686:194-202.

50 Yan, H., Zhang, J., Wen, J. Wang, Y., Niu, W., Teng, Z., Zhao, T., Dai, Y., Zhang , Y., Wang, C., Qin, Y., Xia, G., Zhang, H. (2018) CDC42 in oocytes controls the activation of primordial follicles by regulating PI3K signaling in mice. *BMC Biol.* 16(1):73.

51 Liu, MJ., Sun, AG., Zhao, SG., Liu, H., Ma, SY., Li, M., Huai, YX., Zhao, H., Liu, HB. (2018) Resveratrol improves *in vitro* maturation of oocytes in aged mice and humans. *Fertil. Steril.* 109(5):900-907.

Figure legends

Figure 1 SIRT1 is spatiotemporally expressed in the ovaries of postnatal mice and promotes PF activation

(A) Immunostaining reveals the cellular localization of SIRT1 in the ovaries of postnatal mice. Sections from ovaries on different days were labeled for the presence of SIRT1 (green), the oocyte marker MVH (red) and the nuclear marker DAPI (blue). SIRT1 was expressed in the nuclei of both pGCs and oocytes. Scale bar = 25 μm. **(B)** Relative *Sirt1* expression levels in mouse ovaries on different postnatal days as measured by RT-qPCR and normalized to the levels of *β-actin*. The mRNA levels from 19.0 dpc ovaries were set to 1. **(C)** Western blotting analysis of SIRT1 protein levels in the ovaries of postnatal mice on different days. β-actin served as a loading control.

(D) Representative images showing accelerated initial follicular recruitment in RSV-treated ovaries compared to that in controls. 2 dpp ovaries were cultured for 3 days. The red arrows indicate growing follicles. Scale bar = 100 μm. **(E)** Whole-ovary counting data from serial sections showed a significant increase in the number of growing follicles and an unchanged total number of follicles in RSV-treated ovaries compared to those in control ovaries. 2 dpp ovaries were cultured for 3 days. **(F)** Relative *Sirt*1 mRNA levels in control and *Sirt*1-OE ovaries as measured by RT-qPCR. 1 dpp ovaries were injected with or without *Sirt*1-OE vectors and cultured for 3 days. The expression levels are normalized to those of *β-actin*. The mRNA level of the control ovaries is set as 1. **(G)** Representative images showing that *Sirt1* overexpression accelerated PF activation. 1 dpp ovaries with or without *Sirt*1-OE vectors were cultured for 4 days. The red arrows indicate growing follicles. Scale bar = 100 μm.

Figure 2 SIRT1 facilitates follicular activation independent of its deacetylase activity

(A) Representative images showing accelerated follicular activation in EX527-treated ovaries compared to that in the controls. The red arrows indicate growing follicles.

Scale bar = 50 μm. **(B)** Whole-ovary counting data from serial sections showed a significant increase in the number of growing follicles and a slight but not significant decrease in the total number of follicles in EX527-treated ovaries compared with those in the controls. **(C)** Western blotting analyses showed that EX527 caused an increase in both H3K9ac and SIRT1 protein levels. **(D)** Representative images showing abrogated PF activation in *Sirt1*-KD-treated mouse ovaries compared with that in the controls. The red arrows indicate growing follicles. Scale bar = 100 μm. **(E)** Whole-ovary counting data from serial sections showed a significant decrease in the number of growing follicles and a slight but not significant increase in the total number of follicles in *Sirt1*-KD-treated ovaries compared with those in the controls. **(F)** Western blotting analyses showed that *Sirt1*-KD caused a decrease in SIRT1 and an increase in H3K9ac protein levels. **(G)** Representative images showing accelerated follicular activation in SIRT1-H355Y-overexpressing ovaries compared to that in the controls. The red arrows indicate growing follicles. Scale bar = 50 μm. **(H)** Whole-ovary counting data from serial sections showed a significant increase in the number of growing follicles and a slight but not significant decrease in the total number of germ cells in the SIRT1-H355Y-overexpressing ovaries compared with those in the controls. **(I)** Western blotting analyses showed that SIRT1-H355Y overexpression induced an increase in SIRT1 protein levels but that H3K9ac was unchanged. β-actin served as a loading control.

Figure 3 SIRT1 affects the mRNA expression of initial follicular recruitment-related genes

(A-B) Western blotting analysis showed that RSV, EX527, and SIRT1-H355Y had the same effects on the protein levels of molecules related to initial follicular recruitment. β-Actin served as a loading control. **(C-E)** Western blotting analysis of total Foxo3a and p-Foxo3a protein levels in ovaries of control and RSV-, EX527- or SIRT1-H355Y-treated ovaries. B-actin served as a loading control. **(F-G)** Representative images show that both RSV and EX527 facilitated the translocation of Foxo3a from the nucleus (red arrows) to the cytoplasm (white arrows). Scale bar=50

μm. **(H)** Western blotting analysis of related molecules at the protein level in control and *Sirt1*-KD-treated mouse ovaries. β-Actin served as a loading control. **(I)** RT-qPCR analysis of gene expression in control and RSV- and EX527-treated ovaries. The expression levels are normalized to those of *β-actin*. The mRNA level of the control ovaries is set as 1. **(J)** RT-qPCR analysis of gene expression in control and *Sirt1*-KD-treated ovaries. Expression levels were normalized to those observed in the control ovaries.

Figure 4 Function and mechanism of SIRT1 in pregranulosa cells and oocytes

(A) Immunostaining revealed the cellular specificity of the knockdown system in mouse ovaries. Sections from the *Foxl2* promoter-driven or *Gdf9* promoter-driven vector-treated ovaries were labeled for the presence of GFP (green), MVH (red) and DAPI (blue). Scale bar = 50 μm. **(B)** Representative images showing retarded PF activation in *Foxl2-Sirt1*-shRNA- and *Gdf9-Sirt1*-shRNA-treated ovaries compared with that in the controls. The red arrows indicate growing follicles. Scale bar =200 μm. **(C)** RT-qPCR analysis of gene expression in the control and *Foxl2-Sirt1*-shRNA- and *Gdf9-Sirt1*-shRNA-treated ovaries. The expression levels are normalized to those of *β-actin*. The mRNA level of the control ovaries is set as 1. **(D)** RT-qPCR analysis of gene expression in oocytes and somatic cells from RSV-treated ovaries. The expression levels are normalized to those of *β-actin*. The mRNA level of the control ovaries is set as 1.

Figure 5 SIRT1 binds to the promoters of *Akt1* and *mTOR*

(A) Schematic diagram of the structures of the *Akt1* and *mTOR* promoters. Each rectangle denotes approximately 200 bp. Blue rectangles represent the *Akt1* and *mTOR* promoter-binding sequences for SIRT1. **(B)** ChIP-qPCR analysis showed that SIRT1 directly occupied the promoters of *Akt1* and *mTOR*. Data are presented as the fold change compared to IgG-enriched DNA fragments. **(C)** ChIP-qPCR analysis showed that SIRT1 weakly bound to the promoters of *Pten* and *Tsc1*. Data are presented as the fold change compared to IgG-enriched DNA fragments.

Figure 6 Transient RSV treatment facilitates follicular development in IVA of the mouse ovary

(A-B) Western blotting analysis of the protein levels of related molecules in the control and RSV-treated mouse ovaries. 5 dpp or 35 dpp mouse ovaries were treated with RSV for 30 min, transferred into normal medium and incubated for 12 h. β-actin served as a loading control. **(C-D)** Representative images show that 5 dpp and 35 dpp ovaries exhibited Foxo3a translocation from the nucleus (red arrows) to the cytoplasm (white arrows) after 30 min of incubation in RSV culture medium compared to ovaries incubated in control medium. Scale bar=50 μm. **(E-F)** Representative images show that RSV significantly facilitated follicular activation of 5 dpp and 35 dpp mouse ovaries in IVA experiments. The red arrows indicate growing follicles, and the green arrows indicate PFs. Scale bar=100 μm. **(G-H)** The ovarian size and weight. The 5dpp ovaries were treated with RSV for 30 min and then transplanteded for 14 days. Scale bar=2 mm. **(I)** 5 dpp ovaries incubated with RSV for 30 min and transplanted for 14 days. Hosts received daily i.p. injection of PMSG (2 IU/day) to promote follicle development. Scale bar=200 μm. **(J)** Early embryonic development of RSV-treated oocytes after *in vitro* fertilization. Scale bar=1 μm. **(K)** IVF rate (2-cell/mature oocytes) and blastocyst rate (blastocyst/2-cell).

Figure 7 Transient RSV treatment facilitates follicular development in IVA of the human ovary

(A) Immunostaining revealed the cellular localization of SIRT1 during early follicular development of human ovaries. SIRT1 was expressed in the nuclei of both granulosa cells and oocytes. Scale bar = 25 μm. **(B-C)** RT-qPCR and Western blotting analysis of the levels of related molecules in the control and RSV-treated human ovary fragments. Human ovary fragments were treated with RSV for 30 min, transferred into normal medium and incubated for 12 h. **(D)** Representative images show that RSV significantly facilitated human PF activation in IVA experiments. The green arrows indicate growing follicles, and the red arrows indicate PFs. Scale bar=25 μm.

Figure 8 Working model for the role of SIRT1 during PF initial recruitment

(A) The systematically changed molecules concomitantly promote the activation of PFs in the mouse ovary. In pGCs, SIRT1 directly binds to the promoters of either *mTOR* gene to facilitate transcription, which mediates the transformation of pregranulosa cells to granulosa cells. In oocytes, SIRT1 upregulates the transcription of both *mTOR* and *Akt1* by the same means as in pGCs. **(B)** Transient RSV treatment could stimulate dormant PFs in humans and mice.

Figure 1

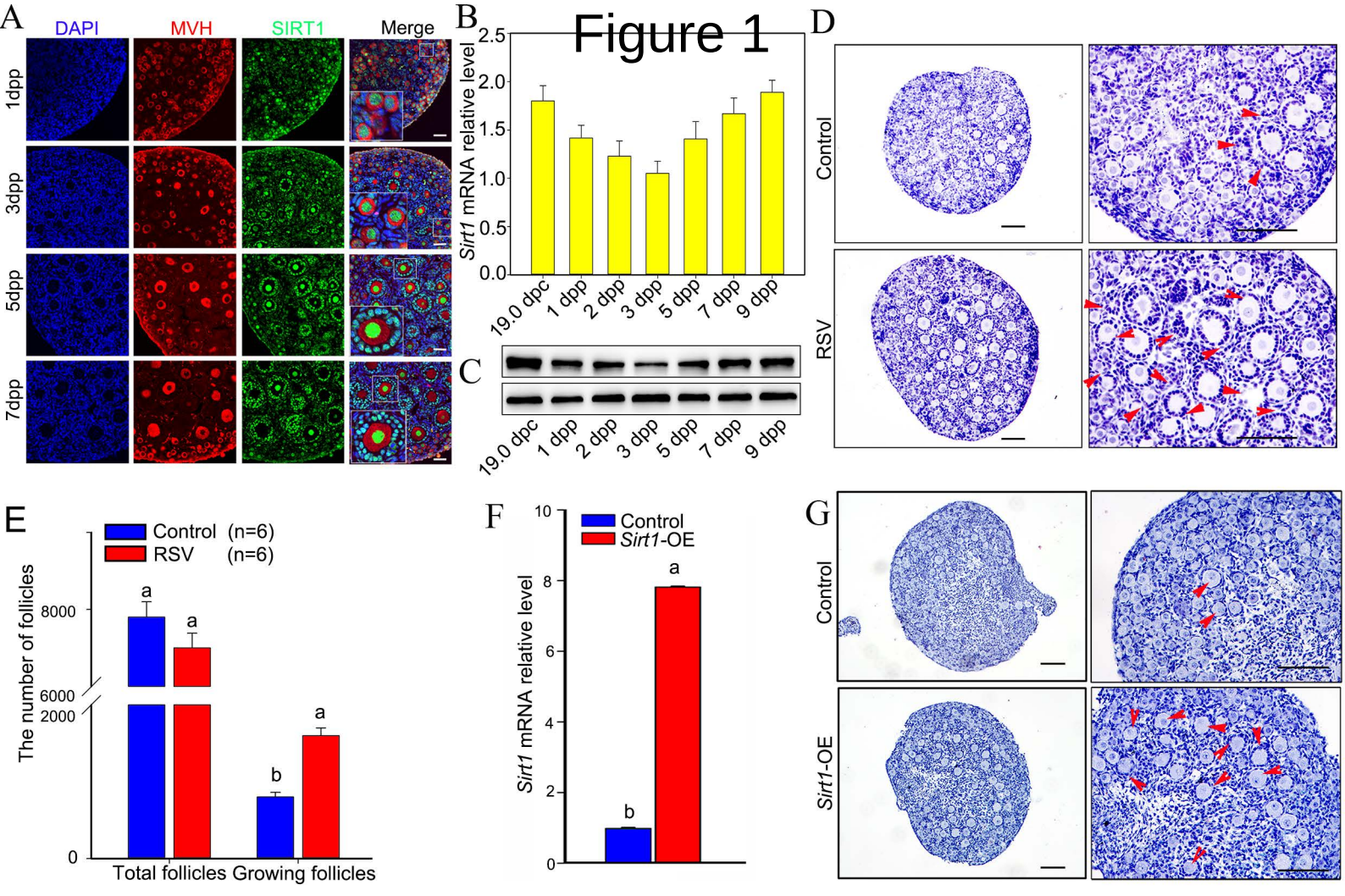
A
DAPI
MVH
SIRT1
Merge
1dpp
3dpp
5dpp
7dpp
B
Sirt1 mRNA relative level
2.5
2.0
1.5
1.0
0.5
0.0
19.0 dpc
1 dpp
2 dpp
3 dpp
5 dpp
7 dpp
9 dpp
C
19.0 dpc
1 dpp
2 dpp
3 dpp
5 dpp
7 dpp
9 dpp
D
Control
RSV
E
Control (n=6)
RSV (n=6)
The number of follicles
8000
6000
2000
0
a
a
b
a
Total follicles
Growing follicles
F
Control
Sirt1-OE
Sirt1 mRNA relative level
10
8
6
4
2
0
a
b
G
Control
Sirt1-OE

Figure2

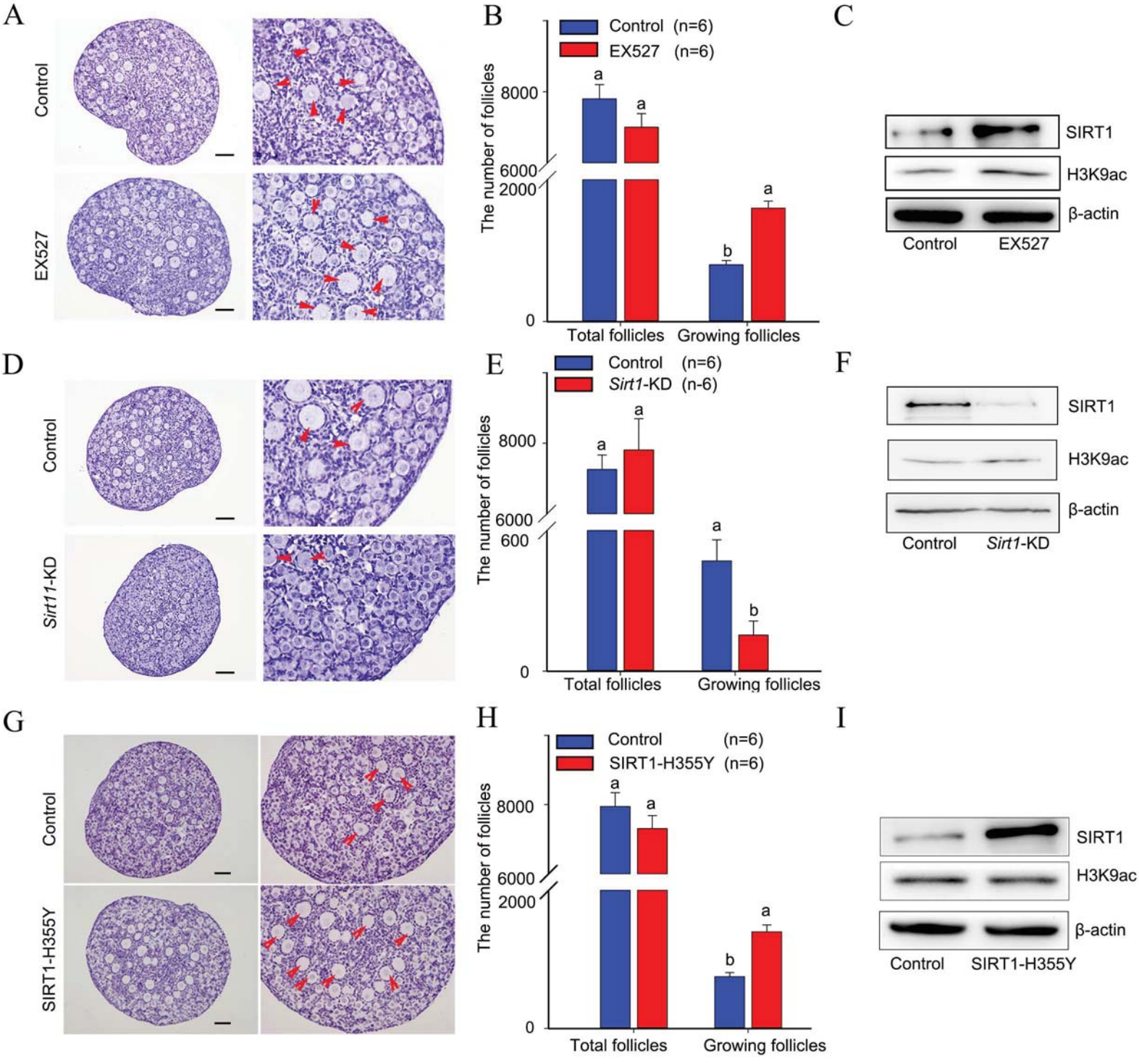
A
Control
EX527
B
Control (n=6)
EX527 (n=6)
The number of follicles
8000
6000
2000
0
a
a
b
a
Total follicles
Growing follicles
C
SIRT1
H3K9ac
β-actin
Control
EX527
D
Control
Sirt11-KD
E
Control (n=6)
Sirt1-KD (n-6)
The number of follicles
8000
6000
600
0
a
a
a
b
Total follicles
Growing follicles
F
SIRT1
H3K9ac
β-actin
Control
Sirt1-KD
G
Control
SIRT1-H355Y
H
Control (n=6)
SIRT1-H355Y (n=6)
The number of follicles
8000
6000
2000
0
a
a
b
a
Total follicles
Growing follicles
I
SIRT1
H3K9ac
β-actin
Control
SIRT1-H355Y

Figure 3

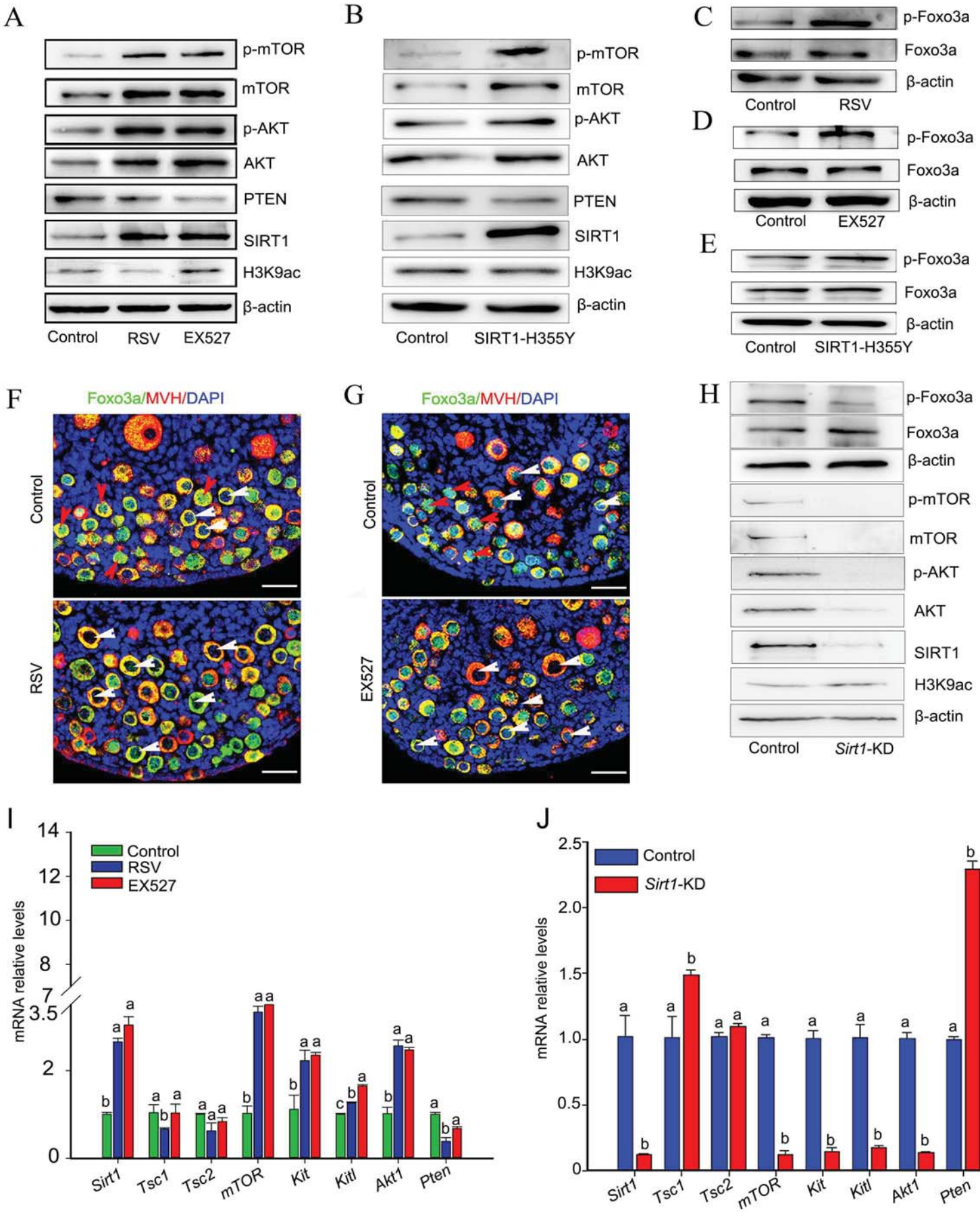
A
p-mTOR
mTOR
p-AKT
AKT
PTEN
SIRT1
H3K9ac
β-actin
Control
RSV
EX527
B
p-mTOR
mTOR
p-AKT
AKT
PTEN
SIRT1
H3K9ac
β-actin
Control
SIRT1-H355Y
C
p-Foxo3a
Foxo3a
β-actin
Control
RSV
D
p-Foxo3a
Foxo3a
β-actin
Control
EX527
E
p-Foxo3a
Foxo3a
β-actin
Control
SIRT1-H355Y
F
Foxo3a/MVH/DAPI
Control
RSV
G
Foxo3a/MVH/DAPI
Control
EX527
H
p-Foxo3a
Foxo3a
β-actin
p-mTOR
mTOR
p-AKT
AKT
SIRT1
H3K9ac
β-actin
Control
Sirt1-KD
I
mRNA relative levels
Control
RSV
EX527
Sirt1
Tsc1
Tsc2
mTOR
Kit
Kitl
Akt1
Pten
J
mRNA relative levels
Control
Sirt1-KD
Sirt1
Tsc1
Tsc2
mTOR
Kit
Kitl
Akt1
Pten

Figure 4

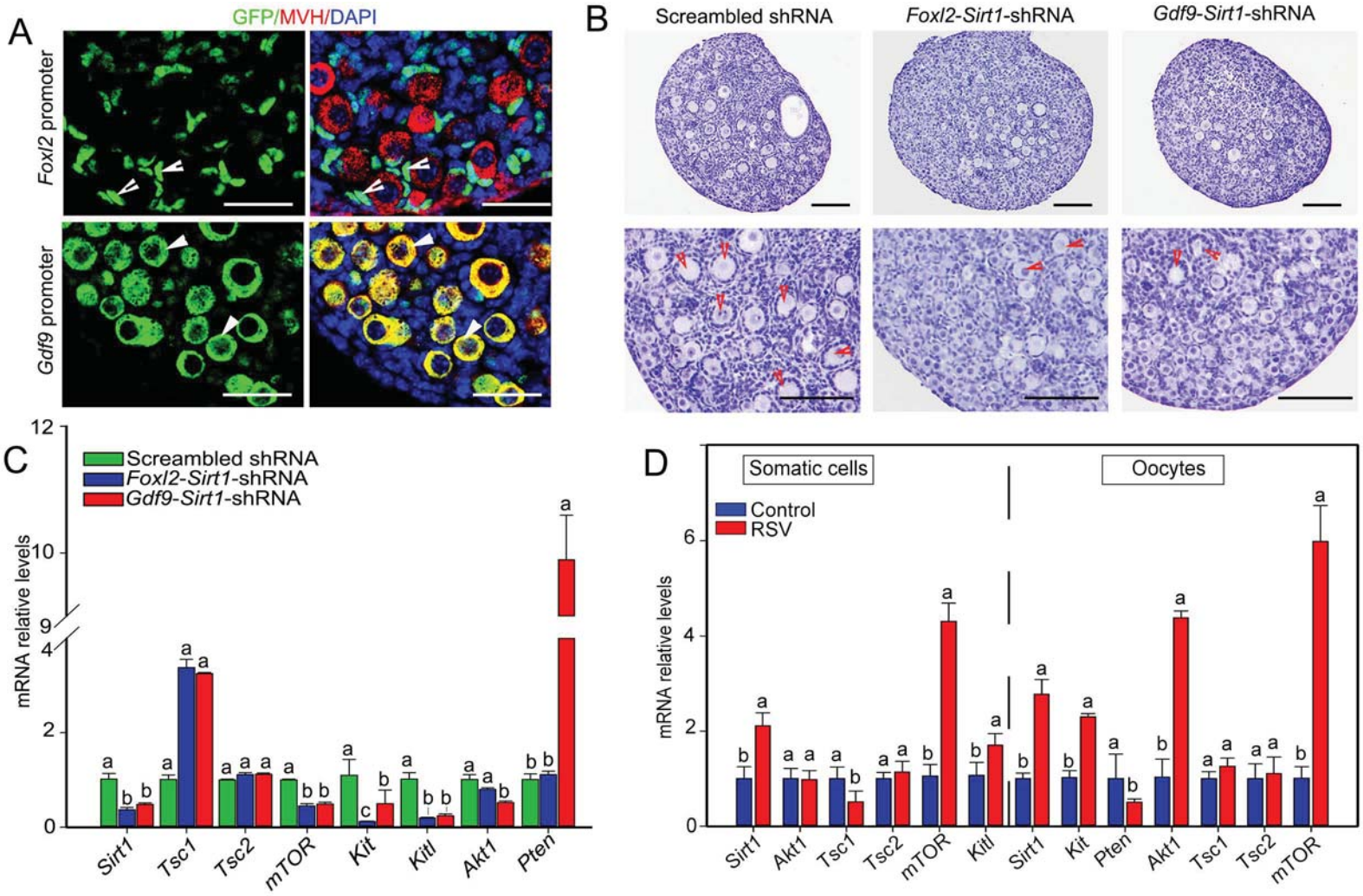
A
GFP/MVH/DAPI
Foxl2 promoter
Gdf9 promoter
B
Screambled shRNA
Foxl2-Sirt1-shRNA
Gdf9-Sirt1-shRNA
C
Screambled shRNA
Foxl2-Sirt1-shRNA
Gdf9-Sirt1-shRNA
mRNA relative levels
Sirt1
Tsc1
Tsc2
mTOR
Kit
Kitl
Akt1
Pten
D
Somatic cells
Oocytes
Control
RSV
mRNA relative levels
Sirt1
Akt1
Tsc1
Tsc2
mTOR
Kitl
Sirt1
Kit
Pten
Akt1
Tsc1
Tsc2
mTOR

Figure 5

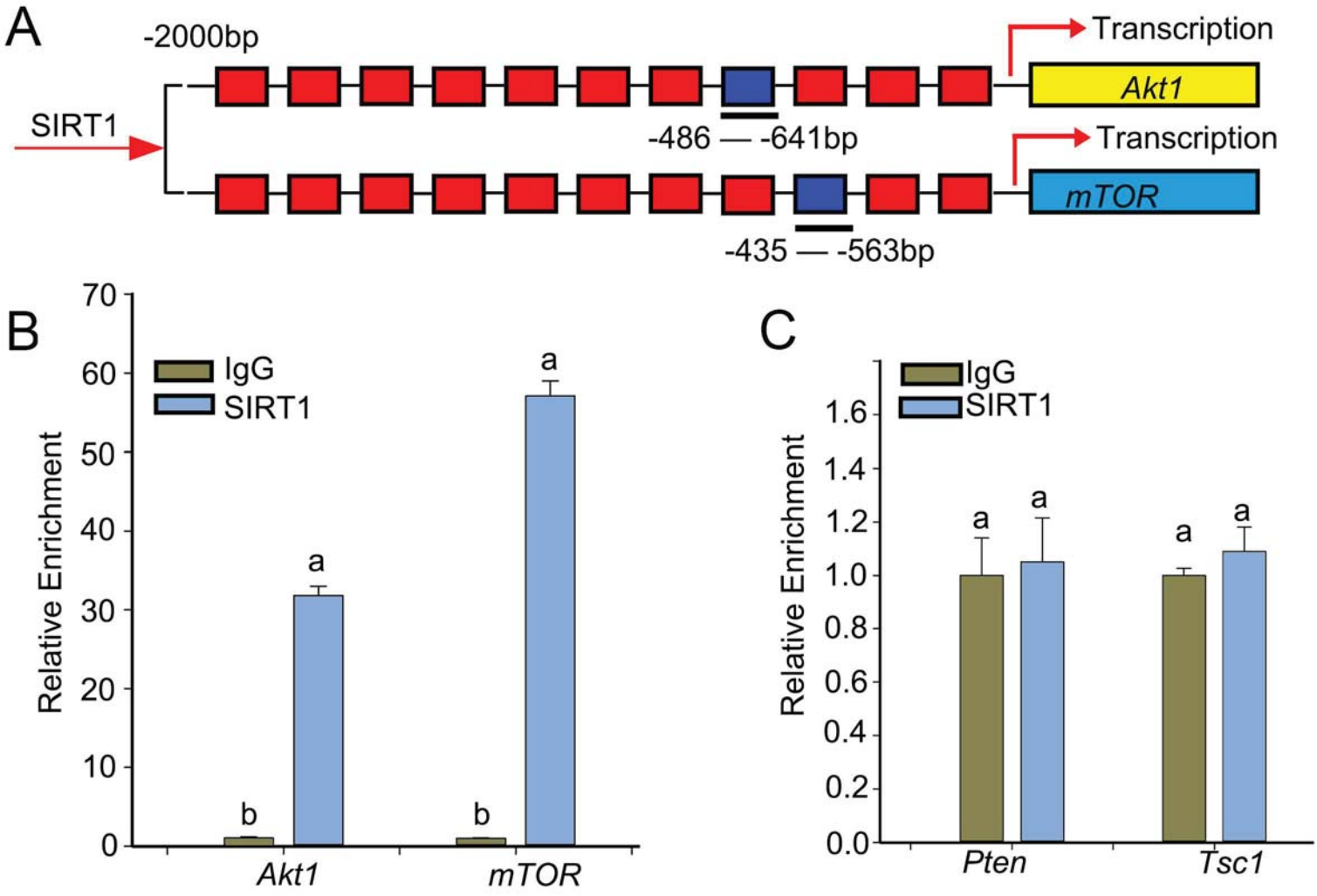
A
-2000bp
SIRT1
Transcription
Akt1
-486 — -641bp
Transcription
mTOR
-435 — -563bp
B
IgG
SIRT1
Relative Enrichment
70
60
50
40
30
20
10
0
a
b
a
b
Akt1
mTOR
C
IgG
SIRT1
Relative Enrichment
1.6
1.4
1.2
1.0
0.8
0.6
0.4
0.2
0.0
a
a
a
a
Pten
Tsc1

Figure 6

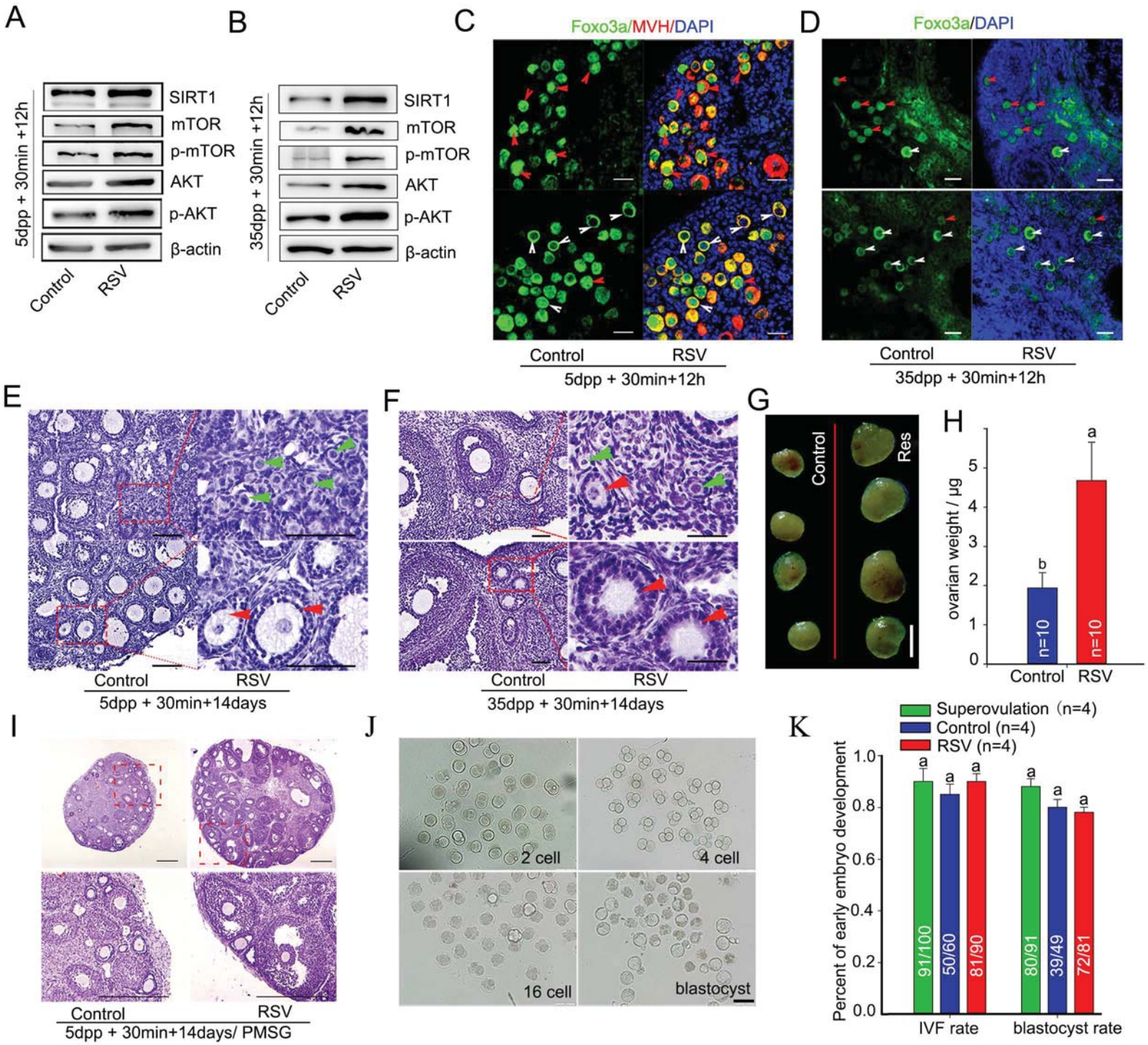
A
5dpp + 30min +12h
SIRT1
mTOR
p-mTOR
AKT
p-AKT
β-actin
Control
RSV
B
35dpp + 30min +12h
SIRT1
mTOR
p-mTOR
AKT
p-AKT
β-actin
Control
RSV
C
Foxo3a/MVH/DAPI
Control
RSV
5dpp + 30min+12h
D
Foxo3a/DAPI
Control
RSV
35dpp + 30min+12h
E
Control
RSV
5dpp + 30min+14days
F
Control
RSV
35dpp + 30min+14days
G
Control
Res
H
ovarian weight / μg
b
a
n=10
n=10
Control
RSV
I
Control
RSV
5dpp + 30min+14days/ PMSG
J
2 cell
4 cell
16 cell
blastocyst
K
Superovulation (n=4)
Control (n=4)
RSV (n=4)
Percent of early embryo development
91/100
50/60
81/90
80/91
39/49
72/81
IVF rate
blastocyst rate

Figure 7

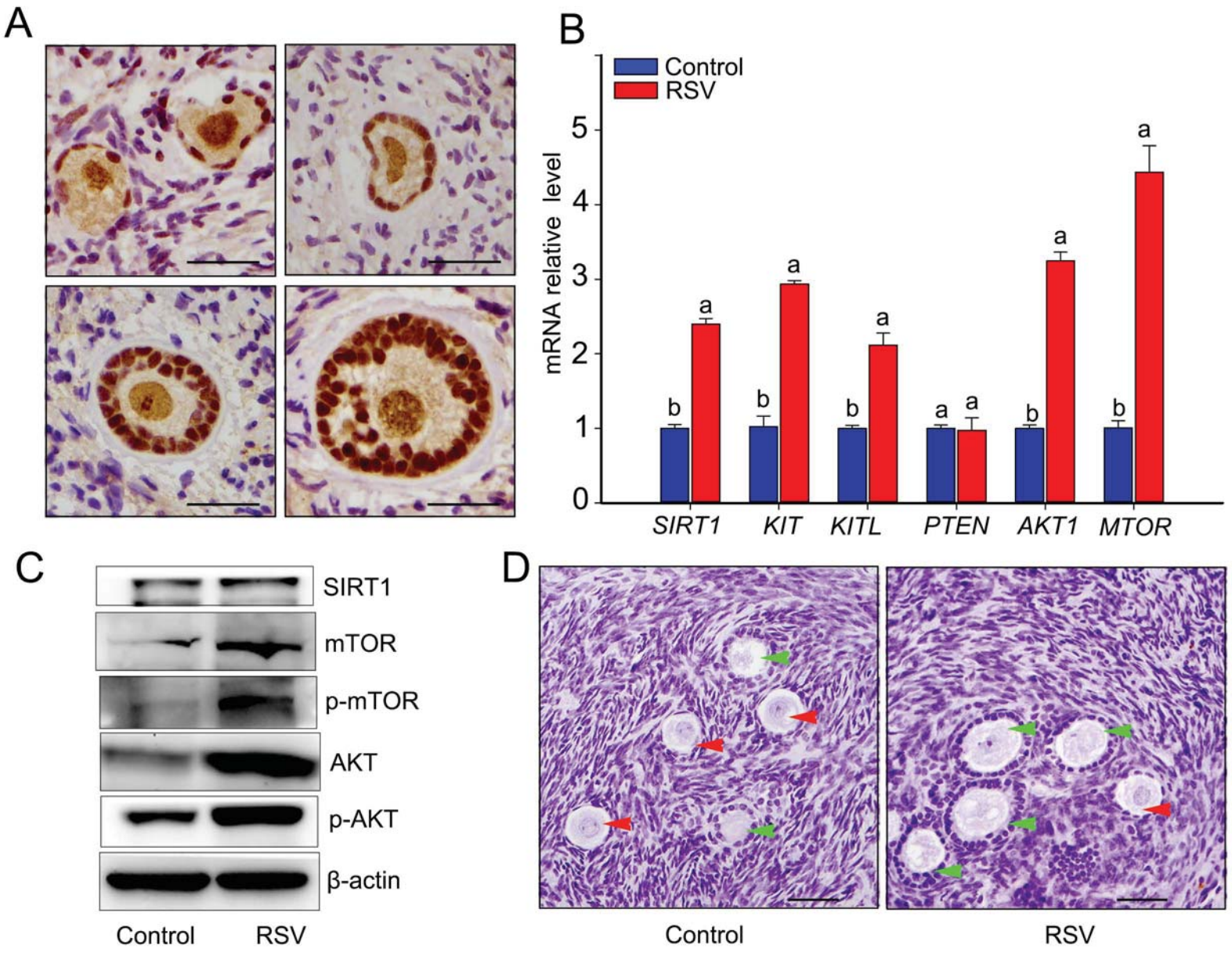
A
B
Control
RSV
mRNA relative level
0
1
2
3
4
5
a
b
SIRT1
KIT
KITL
PTEN
AKT1
MTOR
C
SIRT1
mTOR
p-mTOR
AKT
p-AKT
β-actin
Control
RSV
D
Control
RSV

Figure 8

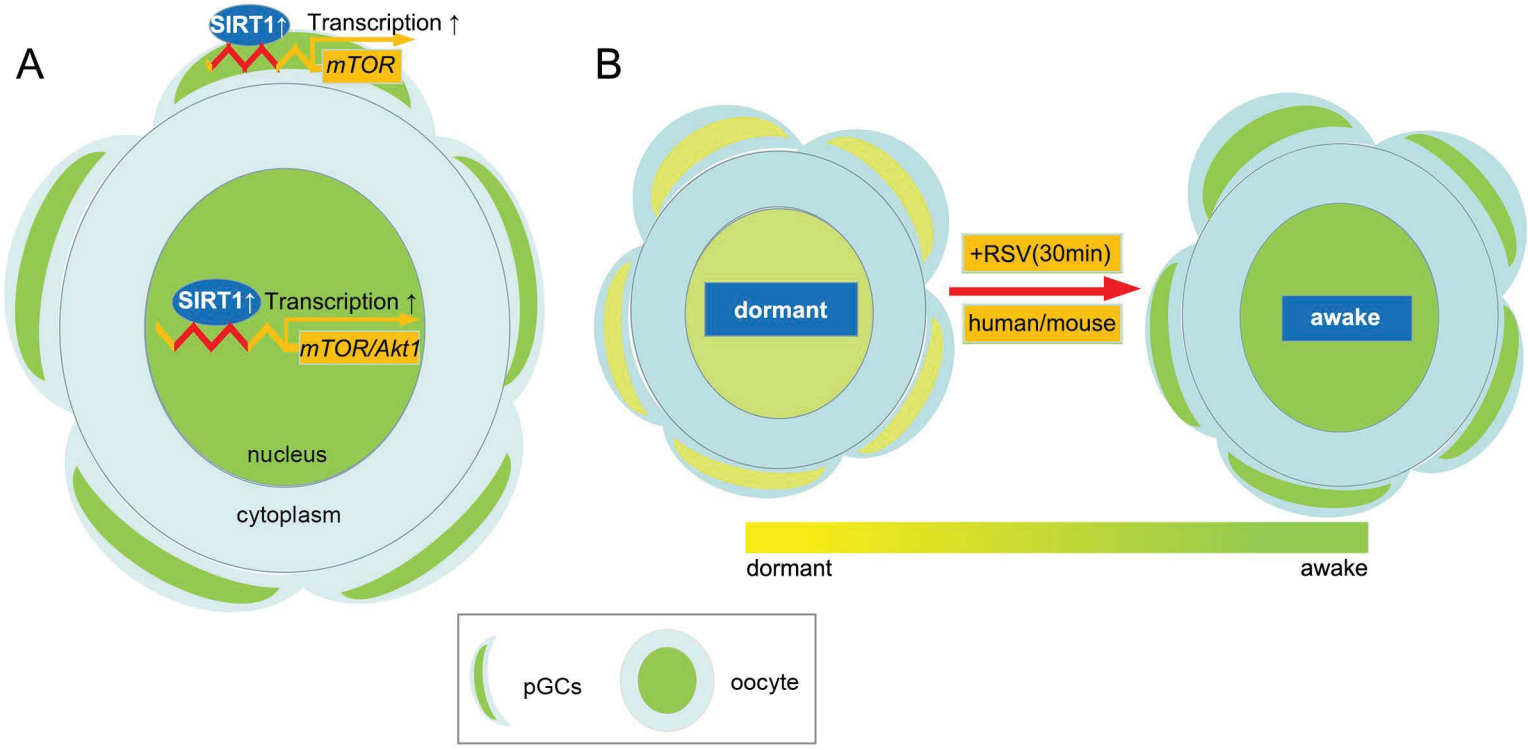
A
SIRT1↑
Transcription ↑
mTOR
SIRT1↑
Transcription ↑
mTOR/Akt1
nucleus
cytoplasm
B
dormant
+RSV(30min)
human/mouse
awake
dormant
awake
pGCs
oocyte